

Multisensor Adaptive Control System for IoT-Empowered Smart Lighting with Oblivious Mobile Sensors

AREG KARAPETYAN, Masdar Institute, Khalifa University, and Research Institute for Mathematical Sciences (RIMS), Kyoto University

SID CHI-KIN CHAU, Australian National University

KHALED ELBASSIONI, SYAFIQ KAMARUL AZMAN, and MAJID KHONJI, Masdar Institute, Khalifa University

The Internet-of-Things (IoT) has engendered a new paradigm of integrated sensing and actuation systems for intelligent monitoring and control of smart homes and buildings. One viable manifestation is that of IoT-empowered smart lighting systems, which rely on the interplay between smart light bulbs (equipped with controllable LED devices and wireless connectivity) and mobile sensors (possibly embedded in users' wearable devices such as smart watches, spectacles, and gadgets) to provide automated illuminance control functions tailored to users' preferences (e.g., of brightness, color intensity, or color temperature). Typically, practical deployment of these systems precludes the adoption of sophisticated but costly location-aware sensors capable of accurately mapping out the details of a dynamic operational environment. Instead, cheap *oblivious mobile sensors* are often utilized, which are plagued with uncertainty in their relative locations to sensors and light bulbs. The imposed volatility, in turn, impedes the design of effective smart lighting systems for uncertain indoor environments with multiple sensors and light bulbs. With this in view, the present article sheds light on the adaptive control algorithms and modeling of such systems. First, a general model formulation of an oblivious multisensor illuminance control problem is proposed, yielding a robust framework agnostic to a dynamic surrounding environment and time-varying background light sources. Under this model, we devise efficient algorithms inducing continuous adaptive lighting control that minimizes energy consumption of light bulbs while meeting users' preferences. The algorithms are then studied under extensive empirical evaluations in a proof-of-concept smart lighting testbed featuring LIFX programmable bulbs and smartphones (deployed as light sensing units). Lastly, we conclude by discussing the potential improvements in hardware development and highlighting promising directions for future work.

CCS Concepts: • **Human-centered computing** → *Ambient intelligence; Ubiquitous and mobile computing*; • **Theory of computation** → *Stochastic control and optimization; Mathematical optimization; Online learning algorithms*; • **Computing methodologies** → *Optimization algorithms*; • **Computer systems organization** → *Sensors and actuators*; • **Mathematics of computing** → *Simulated annealing*; • **Applied computing** → *Engineering*; • **Hardware** → *Sensor devices and platforms*;

This is an extended version of a prior conference paper that appeared in ACM BuildSys 2018 [9].

Authors' addresses: A. Karapetyan, Masdar Institute, Khalifa University, Abu Dhabi, UAE, Research Institute for Mathematical Sciences (RIMS), Kyoto University, Kyoto 606-8502, Japan; email: akarapetyan@masdar.ac.ae; S. C.-K. Chau, Australian National University, Canberra, Australia; email: sid.chau@anu.edu.au; K. Elbassioni, S. K. Azman, and M. Khonji, Masdar Institute, Khalifa University, Abu Dhabi, UAE; emails: kelbassioni@masdar.ac.ae, muhammad.azman@ku.ac.ae, mkhonji@masdar.ac.ae.

Permission to make digital or hard copies of all or part of this work for personal or classroom use is granted without fee provided that copies are not made or distributed for profit or commercial advantage and that copies bear this notice and the full citation on the first page. Copyrights for components of this work owned by others than the author(s) must be honored. Abstracting with credit is permitted. To copy otherwise, or republish, to post on servers or to redistribute to lists, requires prior specific permission and/or a fee. Request permissions from permissions@acm.org.

© 2019 Copyright held by the owner/author(s). Publication rights licensed to ACM.

1550-4859/2019/12-ART11 \$15.00

<https://doi.org/10.1145/3369392>

Additional Key Words and Phrases: Smart lighting control system, oblivious mobile sensors, Internet-of-Things, illuminance control algorithm, wearable computing

ACM Reference format:

Areg Karapetyan, Sid Chi-Kin Chau, Khaled Elbassioni, Syafiq Kamarul Azman, and Majid Khonji. 2019. Multisensor Adaptive Control System for IoT-Empowered Smart Lighting with Oblivious Mobile Sensors. *ACM Trans. Sen. Netw.* 16, 1, Article 11 (December 2019), 21 pages.

<https://doi.org/10.1145/3369392>

1 INTRODUCTION

The prevailing trend of the Internet-of-Things (IoT) is bolstered by the elevated needs for ubiquitous computational intelligence embedded in diverse facilities and infrastructures. A vivid example is in the area of smart homes and buildings, whereby automated control and management systems, using IoT frameworks, regulate appliances and facilities to enhance user comfort and energy efficiency. In keeping with this trend, modern lighting systems are witnessing a drastic departure from conventional incandescent lights to embrace the energy-efficient LED technology, which supports a wider range of reconfigurable brightness levels and colors. These controllable LED devices often come integrated with system-on-a-chip to provide local computation and wireless connectivity supporting mainstream network protocols (e.g., WiFi, ZigBee), thereby ushering in a new class of IoT devices, known as *smart light bulbs* (e.g., Philips Hue, LIFX). In the future, the advances in OLED technology will enable smart luminaries to support a more vibrant color spectrum in flexible form factors that can be integrated with our environment seamlessly, such as being embedded in furniture, decorations, and sculptures, for supporting artistic interior designs and novel infotainment applications. Accordingly, given their increasing affordability and effectiveness in simulating natural light, smart light bulbs are becoming an integral constituent of modern buildings and smart homes.

Meanwhile, an IoT device requires a close integration of sensing and control technology to support advanced applications in dynamic environments. In more sophisticated settings of illuminance management, smart light bulbs will need to incorporate the sensing data from a manifold of wearable/mobile gadgets, such as smartphones, smart watches, wristbands, smart clothes, and spectacles. Furthermore, the development in sensing technologies will allow for lightweight, low-powered, and cost-effective mobile sensors that can be embedded in all forms of wearable devices. Thus, employed in tandem with these sensors, smart luminaries can enable a broad spectrum of novel interactive lighting applications (e.g., a personalizable lighting system that synchronizes with events and activities).

Nevertheless, the novel illuminance management applications considering flexible configurability, dynamic environments, and heterogeneous users' preferences pose unprecedented challenges, effectively rendering the traditional user-operated approach largely futile [22, 23]. Therefore, *IoT-empowered smart lighting systems* demand a novel means of automated control capable of adapting to dynamic surrounding environments while catering for heterogeneous contexts and user preferences in real time. To this end, it needs a tight interplay between wireless controllable smart light bulbs and mobile sensors to continuously adjust the illuminance configurations (e.g., brightness, color intensity, and color temperature) in response to deviations in environmental parameters and users' behavior. An example scenario of desirable smart lighting system is illustrated in Figure 1. On one hand, multiple mobile sensors (embedded in wearable devices like smart watches and spectacles) are utilized to measure the local illuminance close to the end-users. On the other hand, smart luminaries, upon receiving these measurements, coordinate with each other to determine

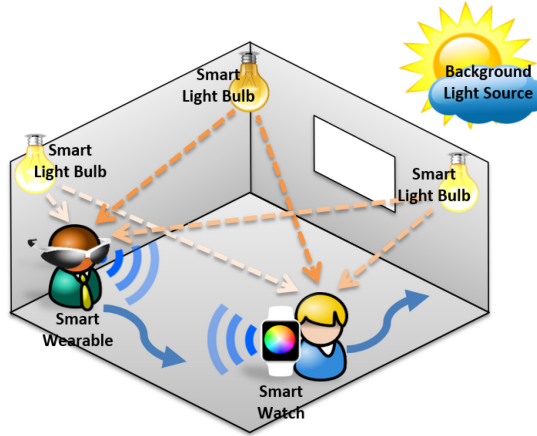


Fig. 1. An example scenario of an IoT-empowered smart lighting system, where mobile sensors in smart wearable devices are broadcasting local illuminance measurements, and smart light bulbs are coordinating with each other to modulate their brightness levels based on the readings.

the appropriate local illuminance configurations to meet users' preferences at the lowest overall energy consumption.

Automated illuminance control can be achieved through various approaches. For instance, one can resort to computer vision using cameras to estimate users' positions and the required illuminance level. Yet, camera placement and maintaining its line of sight could be challenging in the presence of obstacles. Moreover, distinguishing occupants among other objects moving in the scene (e.g., robotic vacuum cleaner or warehouse robots) might prove onerous and often inaccurate. Alternatively, one can utilize advanced location-aware sensors, with indoor localization technology, that can map out the illuminance distribution relative to the locations of light bulbs. However, practical deployment usually precludes involving these sophisticated sensors for financial reasons. Besides, they are still susceptible to challenges from shadowing by obstacles and influences of background light sources. In this work, we pursue a simple yet effective solution for IoT-empowered smart lighting systems. The employed setup involves cheap *oblivious mobile sensors* that measure the perceived illuminance level, without any further information concerning locations, users, or the environment. The key contribution lies in providing a reliable and resilient automated lighting control framework with only oblivious mobile sensors. Particularly, we are interested in the following desirable attributes of smart lighting systems:

- **Dynamic Illuminance without Localization:** Oblivious mobile sensors cannot provide sufficient information to model the detailed illuminance effects of light bulbs in the surrounding environment. The target smart lighting system should allow handling multiple light bulbs, various sources of background light (e.g., the sun, outdoor light sources), and shadows of obstacles that affect user-perceived illuminance in a complicated manner.
- **Ad Hoc Device Management:** An efficient smart lighting system should operate smoothly in ad hoc environments while coping with dynamic addition or removal of devices, including smart light bulbs and mobile sensors. Additionally, all smart light bulbs and mobile sensors should be able to operate with minimal setup process.
- **Computationally Conducive Control Algorithms:** Characteristically in IoT devices, smart light bulbs and mobile sensors are simple portable electronics, and thus do not

possess much computational power. Hence, desirable illuminance control algorithms should be computationally parsimonious and easy to implement in these low-tech IoT devices.

Taking into consideration these properties, we first establish a general model capturing an oblivious multisensor illuminance control problem, which requires no further assumptions or *a priori* knowledge of the dynamic operational environment. Importantly, this model serves as a unifying framework for a number of oblivious multisensor control problems, such as *environmental sensing and control for air quality, sound quality, temperature, and indoor climate* [1]. While the latter are interesting in their own right, here we shall confine the scope solely to the lighting control application.

Under this model, we devise efficient algorithms allowing for continuous adaptive lighting control that minimizes energy consumption of light bulbs and satisfies users' preferences. The basic idea rests on the notion of learning a dynamic environment by random sampling with only a small number of measurements. Unlike standard sampling-based approaches (e.g., those covered in [3, 8, 11, 12]), which entail sizable sampling space and a slow convergence rate, the proposed technique rapidly arrives at near-optimal solutions by reducing the general problem to a subproblem with a simpler and well-defined sampling domain. As a proof-of-concept demonstration, the proposed control algorithms are implemented in a prototype smart lighting testbed system, consisting of programmable smart light bulbs and mobile light sensors in smartphones, deployed in a real-world indoor environment. Empirical results, considering diverse settings and realistic scenarios, are presented to validate the effectiveness and practicality of the proposed control algorithms.

Organization. The remainder of this article is structured as follows. In Section 2, we survey the related literature. Section 3 formulates the model of oblivious multisensor lighting systems and defines the illuminance control problem under study formally. Next, Section 4 elaborates on the devised control algorithms and Section 5 describes the proof-of-concept smart lighting system testbed and experimental setup. Finally, Section 6 presents the result of experiments performed and Section 7 sketches the prospects for further research as well as explores the potential improvements in the hardware development.

2 RELATED WORK

Contemporary research on smart cities and eco-conscious building design has spawned considerable interest in intelligent illuminance management systems. With enhanced functionalities for energy efficiency and adaptive control, these systems offer a broad spectrum of innovative applications. As noted previously, such systems often take into account diverse aspects and practical constraints, such as daylight harvesting, cross-illumination effects, time-varying background light sources, and external factors.

While a comprehensive model involving all aspects of illuminance behavior and the surrounding environment is ideal, it is often impractical, as it requires extensive computations and sophisticated measurements for calibrating the models. Hence, most of the prior literature tackled this problem from one angle or the other, relying on simplifications (by abstracting away some of the constraints) and heuristic algorithms devoid of any performance guarantees.

Along these lines, a centralized wireless networked lighting system is presented in [19, 20] with the goal of maximizing user satisfaction and energy efficiency. However, the employed model is static in nature and hinges upon the availability of *a priori* information on the environmental parameters. The studies in [5, 18] consider static sensors placed on the desks and ceiling to measure the overall lighting condition in a workplace. The ceiling-mounted sensors function as calibration units by detecting occupancy and illuminance at specific spots. Overall, the systems meet user-defined illumination requirements but do not efficiently maximize energy savings as they fix a

preset minimum average illuminance at a work area. A utility-based lighting control strategy was proposed in [16], which trades user comfort for energy reduction. The presented model relies on a simplifying assumption that a small number of users are affected by a single light source and the problem is solved via a heuristic strategy. A similar work in [14] proposes a fast, distributed, stochastic optimization method for achieving correct sensor illuminations but does not account for further energy savings.

In comparison to the aforementioned studies, several other works attempted to attain user-preferred lighting while minimizing power consumption. In [21], a wireless interior lighting system with two satisfaction models is developed, which separately solve for user illuminance preferences and energy expenditure minimization. Therein, an iterative algorithm is presented, which employs linear and nonlinear solvers for the two models. However, a simplified equation for lighting is considered that relaxes the complex interplay of light bulbs and user-perceived illuminance. Recently, in [10] a decentralized algorithm was introduced that balances the lighting while minimizing the energy consumption. Wearable sensing technology was utilized in [23] featuring a context-aware lighting system, which aims to improve user comfort, energy consumption, and system performance. In [15], a sensor system is developed that can monitor and control power usage of appliances (including lights) without supervised training. Based on multisensor fusion and unsupervised machine learning algorithms, the system classifies the appliance events of interest and autonomously associates measured power usage with the respective appliances. However, this study does not directly apply sensor data to lighting control.

3 MODEL AND PROBLEM FORMULATION

This section formulates a general mathematical model for an oblivious multisensor illuminance management problem, along with a corresponding adaptive control framework.

3.1 Multisensor Illuminance Model

The proposed model considers n sensors (indexed by the set $\mathcal{N} \triangleq \{1, \dots, n\}$) and m light bulbs (indexed by the set $\mathcal{M} \triangleq \{1, \dots, m\}$) procured by a controller unit over a decision horizon $\mathcal{T} \triangleq \{1, \dots, T\}$ discretized into T equal periods. Denote by x_i^t the brightness level¹ (which is parameterized by the input power) of the i th light bulb at time $t \in \mathcal{T}$. We shall simply write x_i , without referring to a particular time slot. Let $f_{i,j}^t(x_i^t)$ be an abstract function mapping the input power of the i th light bulb to the recorded illuminance measurement at the j th sensor at time t . Note that a sensor *can only detect the aggregate illuminance level* from all the light bulbs and sources (i.e., $\sum_{i=1}^m f_{i,j}^t(x_i^t)$) unless they all are intentionally switched off. Hence, $f_{i,j}^t(x_i^t)$, in a sense, quantifies the portion the i th bulb contributes to the cumulative illuminance level measured at the j th sensor.

Importantly, the function $f_{i,j}^t(\cdot)$ depends on the locations of sensors and light bulbs, as well as background light sources and external factors. In other terms, $f_{i,j}^t(\cdot)$ is unknown and time-varying, which essentially captures the complex dependence of a dynamic operational environment. Accordingly, we treat it as a black-box function that is invoked via an *evaluation oracle* (namely, the function values are accessible at queried points only, while the exact function is not known). Additionally, it is supposed that $f_{i,j}^t(\cdot)$ should be a concave function. It is noteworthy that the concavity condition is assumed merely for theoretical tractability of the model and is sufficiently general to encompass a wide range of functions.

From a modeling viewpoint, the choice of mapping functions allows remarkable generality of the model and applicability of the algorithms in diverse settings, thereby eliminating the major

¹ Alternatively, one may consider other properties, such as color intensity or temperature of color.

concerns presented in the related literature. Even so, from an algorithmic perspective, such formulation also presents formidable challenges in tractability.

3.2 Smart Lighting Control Problem

With this model, the *multisensor lighting control problem* (LCP) is defined at time $t \in \mathcal{T}$ by the following optimization problem:

$$(LCP) \quad \min_{(x_i^t)_{i \in M}} \sum_{i=1}^m x_i^t \quad (1)$$

subject to $\sum_{i=1}^m f_{i,j}^t(x_i^t) \geq c_j^t, \text{ for } \forall j \in \mathcal{N}$

$$x_i^t \geq 0, \text{ for } \forall i \in \mathcal{M}, \quad (2)$$

where $(c_j^t)_{j \in \mathcal{N}}$ are users' heterogeneous illuminance preferences and Equation (1) is determined only by a *membership oracle* (i.e., a procedure that, given any point, determines whether or not it belongs to the feasible set). Without loss of generality, assume $c_j^t = 1$ for $\forall j \in \mathcal{N}$ as Equation (1) can be normalized to have 1 in the right-hand side by scaling down both of its sides by c_j^t . By a slight abuse of notation, in what follows we shall occasionally refer to a vector of variables without subscript (e.g., $x^t \triangleq (x_i^t)_{i \in M}$) and denote the aggregate illuminance at the j th sensor by $f_j^t(x^t) \triangleq \sum_{i=1}^m f_{i,j}^t(x_i^t)$.

As such, LCP seeks to minimize the total brightness level (equivalently, the energy consumption) of light bulbs, subject to the local illuminance requirements at each sensor. Evidently, the standard optimization techniques are not amenable to LCP, as its constraints are unknown (due to oblivious sensors). The plausible way to solve LCP is by measuring the aggregate illuminance ($\sum_{i=1}^m f_{i,j}^t(\cdot)$) to learn each function $f_{i,j}^t(\cdot)$ while simultaneously computing the control decisions (x_i^t) .

One viable solution is based on learning and random sampling by a subset of measurements. However, when applied to LCP directly, such methods (e.g., Simulated Annealing algorithm [8]) will typically incur a large sampling space and slow convergence rate. Against this backdrop, we present an efficient reduction to transform LCP to an equivalent problem with a simpler feasibility region, allowing a more efficient and rapid way of sampling.

In particular, LCP can be first decomposed into several subproblems through the following transformation. Let $\mathcal{S}(B) \triangleq \{x \mid \sum_{i=1}^m x_i = B, x_i \geq 0\}$ be a feasible solution with a total brightness level equal to the value B . Then, the subproblem defined for a given B takes the form

$$(LCP2[B]) \quad \max_{x^t, \lambda} \lambda \quad (3)$$

subject to $\sum_{i=1}^m f_{i,j}^t(x_i^t) \geq \lambda, \text{ for } \forall j \in \mathcal{N}$

$$x^t \in \mathcal{S}(B). \quad (4)$$

Denote by $\lambda^*[B]$ the optimal objective value of LCP2[B]. Observe that the original problem LCP is equivalent to finding the smallest B such that $\lambda^*[B] = 1$, and hence, one can solve LCP through binary search on the appropriate value of B for LCP2[B].

Next, each subproblem is further reduced to an easier instance, whose feasibility region is limited to a simplex $\mathcal{S}(B)$. More concretely, we rely on the following well-known duality relation:

$$\lambda^*[B] = \max_{x^t \in \mathcal{S}(B)} \min_{p \in \mathcal{P}} \sum_{j=1}^n p_j \sum_{i=1}^m f_{i,j}^t(x_i^t) = \min_{p \in \mathcal{P}} \max_{x^t \in \mathcal{S}(B)} \sum_{j=1}^n p_j \sum_{i=1}^m f_{i,j}^t(x_i^t), \quad (5)$$

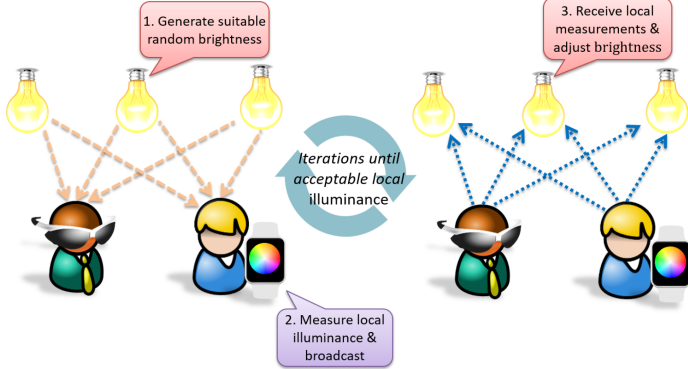


Fig. 2. A conceptual illustration of the bootstrapping control process.

where $\mathcal{P} \triangleq \{p \in \mathbb{R}_+^n \mid \sum_{j=1}^n p_j = 1\}$, and LCP2[B] can be reduced to an equivalent *max-min resource sharing problem* in the form of

$$\lambda^\star[B] = \min\{\Lambda(p) \mid p \in \mathcal{P}\}, \quad (6)$$

where $\Lambda(p) \triangleq \max\{\sum_{j=1}^n p_j \sum_{i=1}^m f_{i,j}^t(x_i^t) \mid x^t \in \mathcal{S}(B)\}$. Hence, if one can tackle Equation (6) efficiently, then one can also solve LCP.

A significant advantage of this approach, as compared to tackling the original problem LCP, is that the solution space in the former case (namely, $\mathcal{S}(B)$) is a regular polytope, which is a well studied subject of optimization. Thus, this method is interesting by itself and can potentially lead to development of efficient algorithms for other oracle-based optimization problems.

4 ADAPTIVE CONTROL ALGORITHMS

The proposed process for smart lighting control is composed of two consecutive stages as follows:

- (1) *Bootstrapping*: Under the paucity of available *a priori* knowledge on the environment (e.g., at the start-up stage or after abrupt changes in environment), the sensors and light bulbs need to solve Equation (6) for setting up the initial configurations.
- (2) *Continual Adjustment*: To ensure continuous adaptive control thereafter, the sensors detect only minor changes in the environment or user preferences in real time and the light bulbs proceed with small adjustments to the present configurations.

Before detailing the algorithms for each stage in the subsequent sections, we first outline the basic ideas underlying each stage.

In the bootstrapping phase, the sensors and light bulbs are unable to rely on any *a priori* knowledge of the environment owing to the uncertainties therein. The high-level concept of the bootstrapping algorithm is illustrated in Figure 2. First, a sequence of brightness levels $\{x', x'', \dots\}$ is generated according to a probability preference model and relayed to the light bulbs. Then, the aggregate illuminance at each sensor $\{(f_j^t(x'))_{j \in N}, (f_j^t(x''))_{j \in N}, \dots\}$ is measured and broadcasted to all light bulbs. Lastly, the light bulbs adjust their brightness levels based on the inferred information from the measurements. This process is applied iteratively until users' illuminance preferences are satisfied, as measured by the sensors.

Admittedly, subtle changes in the environment often occur in practice more frequently than abrupt ones, for example, when users make stationary movements or background light sources (e.g., the sun) gradually change the intensity. In such a scenario, employing the bootstrapping

control with random sampling to learn the resultant environment would be ineffective. Instead, a simple heuristic tuning process, as elaborated in the section to follow, can be invoked to attain the target adjustments more effectively.

In the continual adjustment stage, let Δf_j^t be the change detected in the illuminance measurement of the j th sensor at time instant $t \in \mathcal{T}$. This may incur the violation of Equation (1), implying

$$\Delta f_j^t + \sum_{i=1}^m f_{i,j}^t(x_i^t) < 1.$$

To restore the feasibility, one can progressively perturb the brightness level of each light bulb by a small amount Δx , such that

$$\Delta f_j^t + \sum_{i=1}^m f_{i,j}^t(x_i^t + \Delta x) \geq 1,$$

where Δx is commensurate with the value of the maximum component of $(\Delta f_j)_{j \in \mathcal{N}}$.

4.1 Bootstrapping Algorithm

Recall that the bootstrapping step aims at tackling LCP for determining the optimal brightness configurations $(x_i^t)_{i \in \mathcal{M}}$ of light bulbs such that users' heterogeneous illuminance preferences are satisfied. As noted in Section 3, one computationally efficient approach would be to solve Equation (6) iteratively for each value of B returned by binary search on the interval $[0, \bar{B}]$, where \bar{B} is the expected upper bound on the objective value of LCP. This subsection presents an effective process, as described in Algorithms 1 and 2, which are capable of approximately producing close-to-optimal feasible solutions to LCP.

The proposed method starts with a standard binary search algorithm in Algorithm 1, on the values of B . The latter as a subroutine invokes an adapted variant of the Lagrangian decomposition algorithm introduced in [7]. The execution of this subroutine begins with a trivially feasible solution, then iterates until the relative error μ between the current and previous objective values, defined in step 7, drops below the desired accuracy, characterized by the input parameter η . In a typical iteration, a set of weights $\{p_j\}_{j \in \mathcal{N}}$ corresponding to the set of inequalities in Equation (3) is computed (step 4). These weights are chosen carefully such that the weighted average of the left-hand sides of these inequalities (precisely, $\sum_{j=1}^n p_j \sum_{i=1}^m f_{i,j}^t(x_i^t)$) closely approximates $\min_{j \in \mathcal{N}} \sum_{i=1}^m f_{i,j}^t(x_i^t)$. Based on the assigned weights, the algorithm then, in step 6, selects an \hat{x} among the candidates sampled uniformly from $\mathcal{S}(B)$, which approximately maximizes the mentioned objective. The rationale behind this is that maximizing the minimum of these mapping functions is essentially equivalent to minimizing the violations of users' illuminance preferences. While the intuition has been described in the above, a more theoretically rigorous analysis of the latter claim can be found in the appendix.

Next, Algorithm 2 computes the error μ and the step size τ (steps 7 and 8, respectively), then updates the current solution x as described in step 9. This gives a new feasible solution, thereby concluding the iteration. Note that the step size τ can be altered depending on the application.

An integral part of the above pipeline is the sampling stage in step 6, which requires generating z points from the m -dimensional simplex $\mathcal{S}(B) \triangleq \{x \mid \sum_{i=1}^m x_i = B, x_i \geq 0\}$ uniformly at random, where z is an input parameter of Algorithm 2. In a sense, this is analogous to sampling from a Dirichlet distribution with normalization. As described in [17], this task can be achieved in a different manner, by generating z independent points E_1, E_2, \dots, E_z from an exponential distribution² and then dividing each sample by their sum (i.e., $\sum_{i=1}^z E_i$). The resultant vector is

²By generating a random variable of a uniform distribution on $[0, 1]$ and then computing the negative logarithm.

ALGORITHM 1: $[\epsilon, \eta, \bar{B}, (f_j^t)_{j \in \mathcal{N}}]$

```

1  $B_l \leftarrow 0$ 
2  $B_u \leftarrow \bar{B}$ 
3  $\hat{x}_i \leftarrow \frac{B}{m} \quad \forall i \in \mathcal{M}$ 
4 while  $|\lambda - 1| >= \epsilon$  do
5    $B \leftarrow \left(\frac{B_l + B_u}{2}\right)$ 
6    $(\lambda, (x_i)_{i \in \mathcal{M}}) \leftarrow \text{Algorithm 2}[\eta, B, (f_j^t)_{j \in \mathcal{N}}, \hat{x}, 2m]$ 
7    $\hat{x} \leftarrow x$ 
8   if  $\lambda < 1$  then
9      $B_l \leftarrow B$ 
10  end
11  else
12     $B_u \leftarrow B$ 
13  end
14 end
15 return  $(x_i)_{i \in \mathcal{M}}$ 

```

ALGORITHM 2: $[\eta, B, (f_j^t)_{j \in \mathcal{N}}, x, z]$

```

1  $\mu \leftarrow \frac{\eta}{6} + 1$ 
2 while  $\mu > \frac{\eta}{6}$  do
3   Compute  $\theta$  such that  $\frac{\eta\theta}{6n} \sum_{j=1}^n \frac{1}{f_j^t(x) - \theta} = 1$ .
4    $p_j \leftarrow \frac{\eta}{6n} \frac{\theta}{f_j^t(x) - \theta} \quad \forall j \in \mathcal{N}$ 
5    $\mathcal{S}(B) \triangleq \{(x_i)_{i \in \mathcal{M}} \mid \sum_{i=1}^m x_i = B, x_i \geq 0\}$ 
6   Generate a uniformly random set  $\phi \triangleq \{(x'_i)_{i \in \mathcal{M}}, (x''_i)_{i \in \mathcal{M}}, \dots\}$  with cardinality of  $z$ , where each item  $\in \mathcal{S}(B)$ . Find

```

$$(\hat{x}_i)_{i \in \mathcal{M}} \triangleq \operatorname{argmax}_{y \in \phi} \left\{ \sum_{j=1}^n p_j f_j^t(y) \right\}.$$

```

7    $\mu \leftarrow \frac{\sum_{j=1}^n p_j f_j^t(\hat{x}) - \sum_{j=1}^n p_j f_j^t(x)}{\sum_{j=1}^n p_j f_j^t(\hat{x}) + \sum_{j=1}^n p_j f_j^t(x)}$ 
8    $\tau \leftarrow \frac{\theta\mu}{2n(\sum_{j=1}^n p_j f_j^t(\hat{x}) + \sum_{j=1}^n p_j f_j^t(x))}$ 
9    $x_i \leftarrow (1 - \tau)x_i + \tau\hat{x}_i \quad \forall i \in \mathcal{M}$ 
10 end
11  $\lambda \leftarrow \min_{j \in \mathcal{N}} f_j^t(x)$ 
12 return  $(\lambda, (x_i)_{i \in \mathcal{M}})$ 

```

uniformly distributed over the simplex. As compared to the alternative approaches listed in [17], the proposed procedure requires only $O(zm)$ running time. As with τ , the parameter z can also be adjusted depending on the environment.

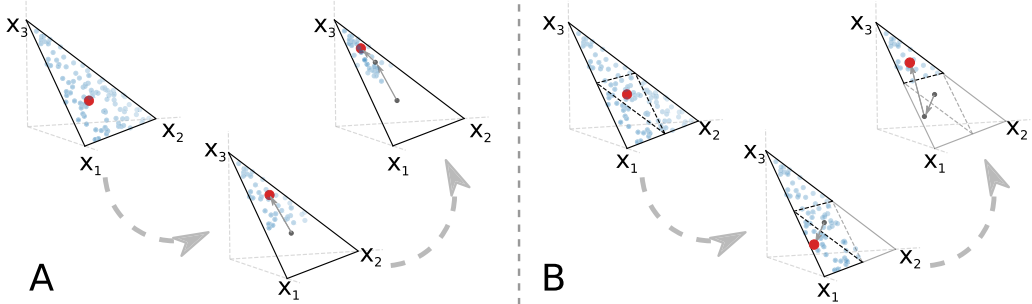


Fig. 3. A high-level illustration of two techniques for alleviating disturbance to users during the sampling routine: (A) Adapting the sampling distribution gradually over iterations. (B) Shrinking the sampling space progressively during each iteration. The red points trace the hypothetical trajectory of the bootstrapping algorithm.

An imperative advantage of Algorithm 2, over standard sampling-based methods, is scalability. While the Simulated Annealing algorithm requires $O^*(m^{4.5})$ operations³ to terminate [8], the empirical evidence suggests that, under judicious choice of input parameters, Algorithm 2 runs notably faster. Observe that, when setting $z = O(m)$, each while loop iteration of Algorithm 2 runs in time $O(nm^2)$. Nevertheless, we remark that the convergence result in [7] for the Lagrangian decomposition algorithm does not necessarily hold for Algorithm 2, which calls for a more elaborate analysis.

4.2 Disturbance-Minimizing Bootstrapping Algorithm

With Algorithm 2 in place, the bootstrapping stage might incur momentary disturbance to users owing to flickering of light bulbs during random sampling. For some applications (e.g., environmental sensing for temperature, sound quality), these distractions are usually of less concern, as their effect on users would be imperceptible, whereas for smart lighting systems, a desirable control algorithm should thwart any intermittent drastic lighting fluctuations, mitigating potential discomfort to users [4]. In light of this, we extend the sampling routine in Algorithm 2 to minimize disturbances during the bootstrapping control.

To this end, one feasible solution would be to amend the sampling distribution during each iteration of the while loop in Algorithm 2, as exemplified in Figure 3(A), specifically, to start with a uniform distribution and alter it gradually to the target distribution (possibly an exponential one) concentrated around the optimum. In this way, the standard deviation of intermediate distributions, and hence the magnitude of lighting fluctuations, is progressively reduced. However, the best-known method (in terms of computational complexity) for sampling from an exponential density over a convex body, namely, the “hit-and-run” algorithm, requires $O^*(m^3)$ running time [13]. Compared to the sampling routine employed in Algorithm 2, the former is computationally prohibitive even for modest input sizes, and hence is impractical.

An alternative approach, as employed in this study and embodied in Algorithm 3, is to truncate the sampling space instead of the distribution itself as depicted in Figure 3(B). That is, after partitioning the feasibility region into a preset number k of roughly equal parts (in a way stated in step 2 of Algorithm 3), in each iteration one of them is discarded, consequently reducing the overall size of the sampling domain. This allows to retain the efficient uniform sampling technique (with only slight modification) leveraged by Algorithm 2 and simultaneously diminish the magnitude of

³The O^* notation hides the polylogarithmic factors.

ALGORITHM 3: $[\eta, B, (f_j^t)_{j \in \mathcal{N}}, x, z, k]$

```

1  $\mu \leftarrow \frac{\eta}{6} + 1; \quad \mathcal{S}(B) \triangleq \{(x_i)_{i \in \mathcal{M}} \mid \sum_{i=1}^m x_i = B, x_i \geq 0\}$ 
2 Partition the simplex  $\mathcal{S}(B)$  into  $k$  roughly equal regions  $\gamma_1, \gamma_2, \dots, \gamma_k$  such that

$$\mathcal{S}(B) = \gamma_1 \cup \gamma_2 \cup \dots \cup \gamma_k.$$


3  $\Gamma \triangleq \{\gamma_1, \gamma_2, \dots, \gamma_k\}$ 
4 while  $\mu > \frac{\eta}{6}$  do
5   Compute  $\theta$  such that  $\frac{\eta\theta}{6n} \sum_{j=1}^n \frac{1}{f_j^t(x) - \theta} = 1$ .
6    $p_j \leftarrow \frac{\eta}{6n} \frac{\theta}{f_j^t(x) - \theta} \quad \forall j \in \mathcal{N}$ 
7   Generate a uniformly random set  $\phi \triangleq \{(x'_i)_{i \in \mathcal{M}}, (x''_i)_{i \in \mathcal{M}}, \dots\}$  with cardinality of  $z$ , where each item  $\in \Gamma$ .
8   Sort the vectors in  $\phi$  by their distance from its first element  $\phi_1$  in an ascending order.
9   Find  $(\hat{x}_i)_{i \in \mathcal{M}} \triangleq \text{argmax}_{y \in \phi} \left\{ \sum_{j=1}^n p_j f_j^t(y) \right\}$ .
10  Compute the Euclidean distances from  $\hat{x}$  to the centroids of each region in  $\Gamma$  and find the index  $v$  of the furthestmost region.
11  if  $|\Gamma| > 1$  then
12     $\Gamma \leftarrow \Gamma \setminus \gamma_v$ 
13  end
14   $\mu \leftarrow \frac{\sum_{j=1}^n p_j f_j^t(\hat{x}) - \sum_{j=1}^n p_j f_j^t(x)}{\sum_{j=1}^n p_j f_j^t(\hat{x}) + \sum_{j=1}^n p_j f_j^t(x)}$ 
15   $\tau \leftarrow \frac{\theta\mu}{2n(\sum_{j=1}^n p_j f_j^t(\hat{x}) + \sum_{j=1}^n p_j f_j^t(x))}$ 
16   $x_i \leftarrow (1 - \tau)x_i + \tau\hat{x}_i \quad \forall i \in \mathcal{M}$ 
17 end
18  $\lambda \leftarrow \min_{j \in \mathcal{N}} f_j^t(x)$ 
19 return  $(\lambda, (x_i)_{i \in \mathcal{M}})$ 

```

lighting fluctuations. Indeed, in order to draw z points uniformly at random from the truncated simplex at a given iteration of the while loop, it suffices to generate at most $O(2^k z)$ points and discard those lying outside the region of interest. Considering k to be $O(1)$, only a constant factor is added to the computational complexity of the algorithm.

Furthermore, rather than probing the generated brightness levels in an arbitrary order, Algorithm 3 chooses the sample nearest to the current one (step 8), thus minimizing the flashing effect between each consecutive pair of samples.

4.3 Continual Adjustment Algorithm

Following the bootstrapping phase, this stage ensures continual adaptive control by periodically monitoring the environment and user preferences for minor deviations. In adapting to these changes, a simple heuristic tuning process, explained below and formalized in Algorithm 4, is adopted.

Given the sensor measurement data at time t , namely, the aggregate illuminance before and after environmental changes (i.e., $(f_j^{t-1}(x^{t-1}))_{j \in \mathcal{N}}$ and $(f_j^t(x^{t-1}))_{j \in \mathcal{N}}$, respectively), Algorithm 4

measures the discrepancy by

$$\Delta f_j^t \leftarrow \min \left\{ f_j^t(x^{t-1}) - f_j^{t-1}(x^{t-1}), 0 \right\}$$

and discards positive Δf_j^t (i.e., when illuminance constraint is satisfied).

Then, it updates the brightness levels based on a simple linear heuristic by

$$x_i^t \leftarrow x_i^{t-1} + \alpha \cdot \max_j |\Delta f_j^t|,$$

where α is a preset parameter characterizing the update step size. If the illuminance constraints remain still unsatisfied (i.e., $f_j^t(x^t) < 1$ for some $j \in \mathcal{N}$), then the update rule is applied iteratively.

As deduced from Algorithm 4, the continual adjustment step runs in time linear in n and m , since $\max_{j \in \mathcal{N}} \frac{\Delta f_j^t}{\alpha}$ is expected to be $O(1)$, and thus is computationally conducive. We remark that in Algorithm 4, other than the linear update rule, nonlinear ones (e.g., quadratic) can be utilized to modulate the pace of updating. Additionally, instead of the parameter α , a specific α_i can be set for each light bulb $i \in \mathcal{M}$.

ALGORITHM 4: $[(f_j^{t-1}(x^{t-1}))_{j \in \mathcal{N}}, (f_j^t(x^{t-1}))_{j \in \mathcal{N}}]$

```

1 for  $j \in \{1, \dots, n\}$  do
2    $\Delta f_j^t \leftarrow \min \left\{ f_j^t(x^{t-1}) - f_j^{t-1}(x^{t-1}), 0 \right\}$ 
3   if  $\Delta f_j^t + f_j^t(x^t) \geq 1$  then
4      $\Delta f_j^t \leftarrow 0$ 
5   end
6 end
7  $x_i^t \leftarrow x_i^{t-1} \quad \forall i \in \mathcal{M}$ 
8 while  $\max_j |\Delta f_j^t| \neq 0$  do
9   for  $i \in \{1, \dots, m\}$  do
10     $x_i^t \leftarrow x_i^t + \alpha \cdot \max_j |\Delta f_j^t|$ 
11   end
12   if  $f_j^t(x^t) \geq 1$  then
13      $\Delta f_j^t \leftarrow 0$ 
14   end
15 end
16 return  $(x_i^t)_{i \in \mathcal{M}}$ 

```

5 EXPERIMENTAL SETUP AND SETTINGS

To validate the efficiency and practicality of the lighting control algorithms derived in Section 4, a proof-of-concept smart lighting testbed is developed and deployed in a real-world indoor environment. This section elaborates on the testbed setup and implementation, scenarios of case studies conducted, and experimental settings.

5.1 Testbed and Deployment Environment

The deployed testbed system, which appears in Figure 4, comprises eight LIFX LED programmable light bulbs (six model A19 and two model BR 30), three Google Nexus 5 smartphones (utilized as light sensors), and a laptop computer. The light bulbs are capable of delivering up to 1,100 lumens at a maximum power output of 11W. Throughout the duration of the experiments, the light

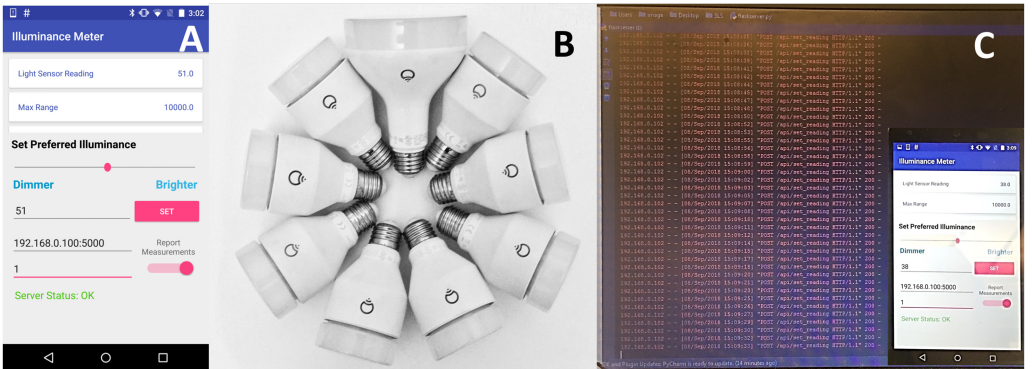


Fig. 4. Components of the deployed smart lighting testbed: (A) Graphical user interface of the developed smartphone application. (B) LIFX Color LED smart light bulbs. (C) Laptop computer with the implementation of proposed control approach.

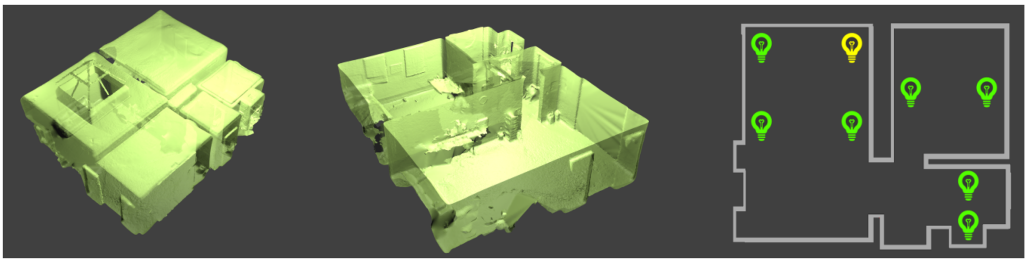


Fig. 5. 3D and 2D sceneries of the testbed environment. The locations of the eight installed LIFX smart light bulbs are marked with icons in the top-view plan. The bulb icon colored yellow was configured to simulate external light disturbances.

bulbs' brightness is managed remotely by the laptop controller via a wireless local network. The laptop hosts a Flask web server written in Python providing a two-way communication channel, through the Lifxlan Python library [6], to acquire the illuminance readings from the smartphones and to relay instructions to the light bulbs. It also performs the computations of the proposed algorithms, taking the smartphones' sensor readings as input. The latter is achieved through an Android application, which was developed in Java programming language and installed on the smartphones.

The left panel of Figure 4 illustrates the Android application at work. The sensor's illuminance reading is displayed at the top of the window along with other details regarding the hardware parameters. Users can set their preferred illuminance level by moving the slider to the left or right should they need a dimmer or brighter setting, respectively, the value of which (in lux) is displayed in the edit box below the slider. Upon decision, the users should press the SET button to trigger the execution of the proposed control algorithm on the laptop's end. The bottom section of the application consists of two inputs fields, namely, the IP address of the laptop controller and the ID of the sensor. To the right of the input fields is a toggle button to initiate the communication between the phone and the controller. Once activated, the smartphone continually broadcasts its illuminance readings every second.

The testbed environment, depicted in Figure 5, occupies the second floor of a residential home, where the light bulbs were installed in three semienclosed areas divided by open doors and short

hallways. Four light bulbs were installed in a living room area (left rectangle of the overhead view in Figure 5) with dimensions of approximately 4m × 4m and a ceiling height of 3.5m. The area featured a pyramid-shaped open ceiling window. Two light bulbs were installed in a bedroom (top left rectangle of the overhead view in Figure 5) of dimensions equal to the living room and the remaining two bulbs were installed in a bathroom (bottom left rectangle of the overhead view in Figure 5) with a ceiling height of 3m and area of 2m × 3m. This environment presents heterogeneous lighting conditions in a sense that some light bulbs may cross-illuminate while others do not.

To test the robustness of the derived algorithms, we simulated an external light disturbance during some of the experiments. Particularly, one light bulb (yellow light bulb icon of the top-view in Figure 5) was randomly flickered at certain points during the course of these experiments while the remaining time was kept on at full brightness. This setting captures abrupt changes in lighting conditions, for example, when users draw the curtains during daytime.

5.2 Lighting Control Scenarios

For a comprehensive evaluation of the proposed algorithms, diverse settings and scenarios were employed considering users' mobility and illuminance preferences and number of sensors and light bulbs. Particularly, the following list details the examined scenarios.

- a) Scenario \mathcal{A} [E1, E1S]: This scenario consists of three light bulbs in the living room with two users. Users' illuminance preferences were held constant while they moved randomly around the room moving toward and away from light bulbs. This scenario also features the simulated external light disturbance explained earlier.
- b) Scenario \mathcal{B} [E2, E2S]: Here, the experiments were carried out in the bedroom area. Two light bulbs were controlled to meet two stationary users' time-varying illuminance preferences.
- c) Scenario C [E3S]: In this scenario, all three rooms described in the previous subsection were involved. The experiment is similar to E1 but with seven light bulbs and three sensors. Each sensor was placed in a different room. Like Scenario \mathcal{A} , this experiment is also subjected to the simulated external light disturbance.

For scenarios \mathcal{A} and \mathcal{B} , during the bootstrapping stage we employ Algorithms 2 and 3 to compare their effectiveness in identical settings. To discern between the results, the experiments with the latter were labeled as E1S and E2S, while those with the former were labeled as E1 and E2. For scenario C, the bootstrapping control is performed with Algorithm 3 in order to test its scalability and the experiment was labeled as E3S.

5.3 Experimental Settings

In all the experiments performed, the smartphones were kept on a surface facing toward the ceiling, although not necessarily directly under a light bulb. We remark that using smartphones as illuminance sensors was a matter of availability rather than a constraint of this experimental setup. In fact, we argue that the setup would yield similar results, if not better, with wearable sensors (e.g., Google Glass, smartwatch, etc.) as such devices capture users' illuminance preferences more accurately.

The experiments were conducted close to sunset time, when sunlight can still be observed, and at night. These two timings represent periods when artificial lighting is necessary, compared to the daytime when natural sunlight was abundant in the testbed environment.

The controller unit in the proposed setup executes either the bootstrapping control to learn the environment or the continuous adjustment algorithm to meet users' lighting requirements rapidly. A major change detected between users' reported preference and the recorded illuminance at the corresponding sensor will invoke the bootstrapping algorithm in order to relearn the

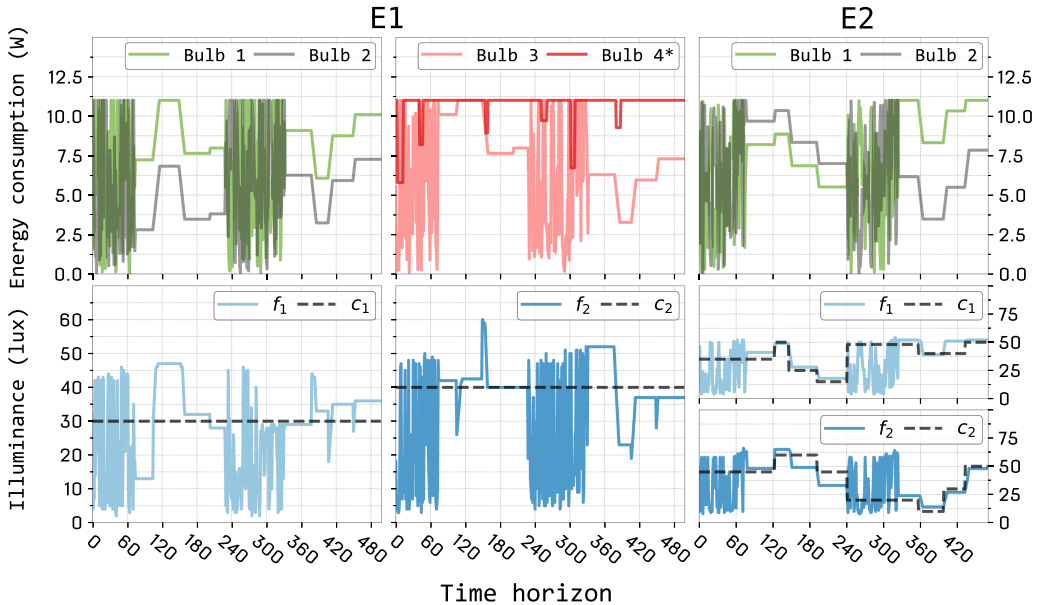


Fig. 6. Energy expenditure of light bulbs, measured illuminance at sensors (f), and users' preferred illuminance (c) over time for experiments E1 and E2 using Algorithm 4 for continual adjustment process and Algorithm 2 for bootstrapping control. Bulb 4, marked with an asterisk, was used to simulate external light disturbances and is not included in the control framework.

environment. Conventionally, this threshold is defined to be strictly greater than 25 lux, below which the continuous adjustment algorithm (Algorithm 4) should be adequate.

For practical purposes, the update step size parameter τ in Algorithms 2 and 3 was set constant, a decision made under extensive empirical experimentation. Also, the parameter k in Algorithm 3, which indicates the number of regions, was set to 3.

6 EVALUATION STUDIES

This section evaluates the effectiveness of the proposed control algorithms through extensive experiments in the deployed smart lighting testbed. The adopted experimental settings and testbed setup reflect the specifications given in Section 5. In the subsections to follow, we present the results, which appear in Figures 6, 7, and 8.

6.1 Smart Lighting with Oblivious Sensors

The results obtained from the first set of experiments, namely, E1 and E2, are depicted in Figure 6. As can be inferred, the proposed approach, when Algorithm 4 was invoked during the continual adjustment stage and Algorithm 2 for bootstrapping, proved successful at minimizing the total power consumption of smart light bulbs without compromising users' illuminance preferences. In E1, the system effectively executed the continual adaptive adjustment algorithm to satisfy users' preferences despite their intensive mobility. Around time horizon 160 in E1, the sudden movement of user 2 toward a light source resulted in a spike in the observed measurements, therein triggering the continual adjustment routine, which rapidly modulated light bulbs' input wattage as to meet the users' lighting requirements. Notice that the proposed approach prevailed despite the adversarial impact of the simulated external light disturbances (the bulb marked with an asterisk in Figure 6). Specifically, subtly steeper descents are evident, as a result of the abrupt dimming, in

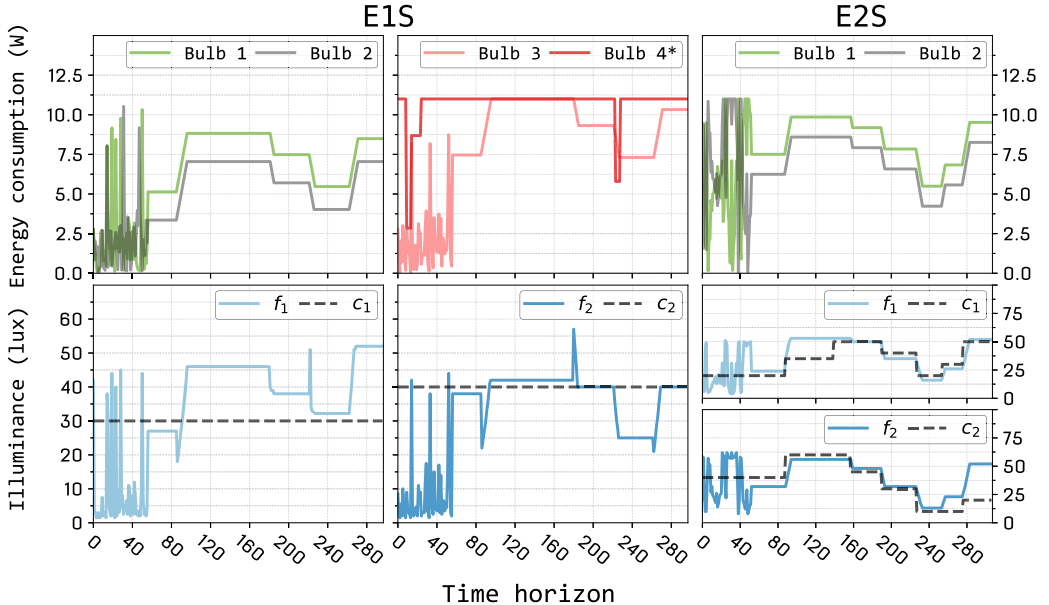


Fig. 7. Energy expenditure of light bulbs, measured illuminance at sensors (f), and users' preferred illuminance (c) over time for experiments E1S and E2S using Algorithm 4 for continual adjustment process and Algorithm 3 for bootstrapping control. Bulb 4, marked with an asterisk, was used to simulate external light disturbances and is not included in the control framework.

E1 around time steps 160 and 375. Similarly, the employed approach also performed well throughout E2 by matching users' heterogeneous requirements consistently without noticeably over- or underilluminating.

Though Algorithm 4 is expedient for small perturbations, it could fail to properly minimize the energy wastage and meet users' conflicting illuminance preferences in the events of significant illuminance variations in the environment. Thus, in E1, when user 1 moved sufficiently far from a light source at around time step 250, dropping the sensor readings from 28 lux to below 5 lux, the controller unit initiated the bootstrapping phase. Also, the bootstrapping control served well in the beginning of experiments E1 and E2, when the system was completely oblivious to the deployment environment.

While the employed control strategy is commendable, it should be noted that the bootstrapping stage is disconcerting as numerous large fluctuations of light bulbs accompany its sampling routine. To the user, this translates to an unsettling period of random flashing of lights, even when smooth lighting transitions are enabled. We remark that it is not necessarily the frequency of these fluctuations but rather the sizable difference in the magnitude of these transitions that brings discomfort. The culprit here is the design of Algorithm 2, where sampling is performed over the entire simplex domain, hence the frequent large changes in the light bulbs' brightness (i.e., each bulb's input wattage takes values from 0% to 100%). As this questions practicality of the developed framework in some applications, as is the case with smart lighting systems, it is vital to minimize the intensity of fluctuations, thereby creating a more visually tolerable user experience. The following subsection presents the results of experiments conducted with Algorithm 3, which circumvents these concerns.

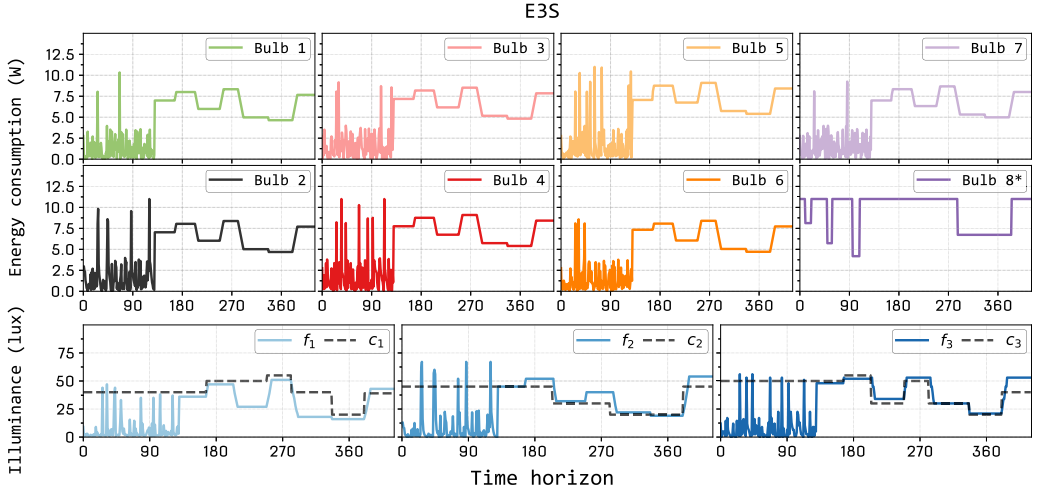


Fig. 8. Energy expenditure of light bulbs, measured illuminance at sensors (f), and users' preferred illuminance (c) over time for experiment E3S using Algorithm 4 for continual adjustment process and Algorithm 3 for bootstrapping control. Bulb 8, marked with an asterisk, was used to simulate external light disturbances and is not included in the control framework.

6.2 Disturbance Minimization

The results of the second set of experiments, namely, E1S, E2S, and E3S, are shown in Figures 7 and 8. It can be observed that, when using Algorithm 3 for the bootstrapping phase, the featured control approach performs comparably in terms of the number of fluctuations at the beginning of the experiment, when the system is exploring the environment. However, the magnitude of fluctuations in E1S and E2S on average is much smaller than that in E1 and E2. For example, as illustrated in Figure 7, in E1S, after an initial fluctuation of about 40 lux, the algorithm zones into a smaller area of the simplex where the sampling domain shrinks, consequently resulting in marginal subsequent fluctuations with a magnitude of around 10 to 20 lux. When observed in reality, the visual disturbances range from slightly perceptible to almost imperceptible. In E1, the fluctuations were oscillating between 0 and 45 lux, resulting in a more compelling change in the perceived illuminance. This reduction in the average range of fluctuations is the hallmark of an algorithm suited for oblivious lighting problems. Importantly, this can be further reduced by considering a certain order of sampling probes in a sense to be clarified in the following section.

As observed from Figures 6 and 7, at time steps around 100 in E1S and 120 in E1, the sensors recorded nearly the same illuminance levels in both experiments (roughly 45 lux at sensor 1 and 40 lux at sensor 2), while the overall input wattage of light bulbs was higher in E1. This is attributed to the timing of experiments; E1S was performed before sunset when mild sunlight leaked into the environment, while E1 was conducted late at night.

The last experiment E3S, whose results are pictured in Figure 8, seeks to investigate the scalability of the proposed approach on a larger-scale instance with seven light bulbs and three sensors. As in previous experiments, the algorithm prevailed in meeting users' heterogeneous illuminance preferences while minimizing the net energy expenditure of smart light bulbs. Also, it displayed robustness when presented with external abrupt light disturbances. In particular, the sharp drop in illuminance brought by Bulb 8 was well handled at time step 280 along with the abrupt rise in illuminance at time step 390. However, the bootstrapping phase witnessed a longer period of fluctuations in E3S as compared to E2S and E1S, signifying that the algorithm explored a larger

sampling space. Despite this, the featured control algorithm managed to reach a solution within an acceptable time frame, thus confirming its scalability in larger problem spaces.

7 DISCUSSIONS

While the deployed testbed prototype demonstrates the empirical effectiveness of the proposed smart lighting control approach, further improvement can be attained, for user comfort and performance, through auxiliary hardware upgrades. This section elaborates on the latter aspect and suggests promising directions for future work.

7.1 Hardware Improvements

In Section 3, an efficient strategy was introduced to attenuate the visual discomfort and disturbance to users during the bootstrapping control phase. Below, we list several possible solutions, on the hardware side, to further enhance user comfort and experience as well as expand the system's functionalities.

- (1) *Improved Sensors and Light Bulbs:* The implemented testbed prototype relies on Android smartphones and LIFX smart light bulbs connected through a wireless local network, whereas it is possible to design specific wearable devices with improved light sensors and a dedicated communication network that have a faster reaction time and refined communication capabilities. This will minimize the latency in data transfer between sensors, smart light bulbs, and the monitoring unit. Moreover, future smart light bulbs are expected to be equipped with improved power electronics, allowing for rapid brightness adjustments, which will further reduce the control lags.
- (2) *Wearable Sensors with Accelerometers:* To improve the performance of the control algorithm, we can incorporate the accelerometer readings in mobile devices that are embedded with light sensors. For example, if there are slower changes in the motion of sensors, then the control system will execute the continual adjustment algorithm at a slow pace. If there are more rapid changes in the motion of sensors, then the continual adjustment algorithm will be executed at a faster pace. In general, it will be an interesting future study to integrate the accelerometer readings in the control system for more effective smart lighting control.

7.2 Color Adjustments

The present study demonstrates the effectiveness of intelligent lighting control system empirically in a real-world environment. However, the featured control approach can also be applied to a more sophisticated setting of multicolor illuminance control [2]. For example, users can set heterogeneous preferences on the *color temperature*. Different colors exhibit distinct radiation effects: reddish colors create a warmer effect to the human eye, while bluish ones colder. It is well known that warmer colors are more pleasant to humans in dim environments, whereas colder colors are better for bright environments. Also, users may have different psychological preferences to color temperature. Hence, given these heterogeneous preferences, the perceived objective would be to coordinate the color and brightness adjustments of smart light bulbs at their lowest possible energy expenditure.

8 CONCLUDING REMARKS

This article studied a practical application of an IoT-empowered sensing and actuation system for smart lighting control with oblivious mobile sensors, which seeks to induce continuous adaptive control in real time without complete knowledge of the dynamic uncertain environment. The

featured system has been implemented in a prototype testbed, using programmable smart light bulbs and light sensors in smartphones, deployed in a real-world indoor environment. We presented a novel model formulation, capturing general oblivious multisensor IoT applications by a generic framework, yielding a robust control framework agnostic to a deployment environment and the associated parameters. With this model, we devised efficient algorithms that minimize the total energy expenditure of smart light bulbs while meeting users' heterogeneous illuminance requirements. The proposed algorithms were applied to the testbed and their effectiveness was validated extensively under diverse settings and scenarios. Lastly, we discussed some potential improvements on the hardware side along with promising directions for future work.

APPENDIX

The appendix sketches the theoretical foundations for Algorithms 2 and 3.

Analytical Underpinnings of the Bootstrapping Algorithms

Recall that Algorithms 2 and 3, in producing close-to-optimal approximately feasible solutions to LCP2[B], seek to tackle its counterpart of the form of

$$\lambda^*[B] = \min\{\Lambda(p) \mid p \in \mathcal{P}\}, \quad (7)$$

where $\Lambda(p) = \max\{\sum_{j=1}^n p_j \sum_{i=1}^m f_{i,j}^t(x_i^t) \mid x^t \in \mathcal{S}(B)\}$ and $\mathcal{P} = \{p \in \mathbb{R}_+^n \mid \sum_{j=1}^n p_j = 1\}$. As mentioned previously, both algorithms borrow from the Lagrangian decomposition scheme of [7]. Accordingly, the proceeding analysis follows closely the lines laid out therein.

The employed decomposition, put simply, is an iterative strategy that approaches LCP2[B] via its Lagrangian dual by computing pairs of vectors p, x successively in the following manner. Given the current $x \in \mathcal{S}(B)$, the algorithm generates a set of weights $p \in \mathcal{P}$ corresponding to the coupling constraints in Equation (3). For this p , it then computes an approximate solution \hat{x} of $\Lambda(p)$ and moves from x to $(1 - \tau)x + \tau\hat{x}$ with a suitable step length $\tau \in (0, 1]$.

The cornerstone of this method relies on attributing to the covering constraints in Equation (3) a *logarithmic potential function* of the form

$$\Phi(\theta, f) = \ln \theta + \frac{\xi}{n} \sum_{j=1}^n \ln(f_j^t(x^t) - \theta), \quad (8)$$

where $\theta \in \mathbb{R}$, $f = (f_j^t)_{j \in \mathcal{N}}$ are variables and ξ is a fixed positive parameter proportionate to the accuracy tolerance η in Algorithms 2 and 3. Note that Φ is well defined for $0 < \theta < \lambda(f) \triangleq \min_{j \in \mathcal{N}} \{f_j^t\}$ and its maximizer $\theta(f)$ emerges from the first-order optimality condition

$$\frac{\xi \theta}{n} \sum_{j=1}^n \frac{1}{f_j^t(x^t) - \theta} = 1, \quad (9)$$

which has a unique solution as its left-hand side is a strictly increasing function of θ . Then the logarithmic dual vector (weights) can be defined as

$$p_j = \frac{\xi}{n} \frac{\theta(f)}{f_j^t(x^t) - \theta(f)} \quad \forall j \in \mathcal{N}, \quad (10)$$

since now $p \in \mathcal{P}$ by Equation (9). On these grounds, the following lemma is formulated.

LEMMA 1 ([7]). Let $\eta \in (0, 1)$, $\xi = \frac{\eta}{6}$ and p be derived from Equation (10) for a given $x \in \mathcal{S}(B)$. Suppose an approximate solution $\hat{x} \in \mathcal{S}(B)$ to $\Lambda(p)$ is computed such that $\sum_{j=1}^n p_j f_j^t(\hat{x}) \geq (1 - \xi)\Lambda(p)$.

If $\mu = \frac{\sum_{j=1}^n p_j f_j^t(\hat{x}) - \sum_{j=1}^n p_j f_j^t(x)}{\sum_{j=1}^n p_j f_j^t(\hat{x}) + \sum_{j=1}^n p_j f_j^t(x)} \leq \xi$, then x is an approximately feasible solution to LCP2[B], satisfying $\sum_{i=1}^m f_{i,j}^t(x) \geq (1 - \eta)\lambda^*[B]$ for $\forall j \in \mathcal{N}$.

PROOF. Rewrite the condition $\mu \leq \xi$ as

$$(1 - \xi) \sum_{j=1}^n p_j f_j^t(\hat{x}) \leq (1 + \xi) \sum_{j=1}^n p_j f_j^t(x). \quad (11)$$

Observe that

$$\sum_{j=1}^n p_j f_j^t(x) = \sum_{j=1}^n \frac{\xi}{n} \frac{\theta(f) f_j^t(x)}{f_j^t(x) - \theta(f)} \quad (12)$$

$$= \frac{\xi \theta(f)}{n} \sum_{j=1}^n \frac{f_j^t(x)}{f_j^t(x) - \theta(f)} \quad (13)$$

$$= \frac{\xi \theta(f)}{n} \sum_{j=1}^n \left(1 + \frac{\theta(f)}{f_j^t(x) - \theta(f)} \right) \quad (14)$$

$$= \xi \theta(f) + \theta(f) \sum_{j=1}^n p_j \quad (15)$$

$$= (1 + \xi) \theta(f). \quad (16)$$

Since $\sum_{j=1}^n p_j f_j^t(\hat{x}) \geq (1 - \xi)\Lambda(p)$, from Equations (11) and (16) it follows that

$$(1 - \xi)^2 \Lambda(p) \leq (1 + \xi)^2 \theta(f). \quad (17)$$

This, in conjunction with the facts that $\theta(f) < \lambda(f)$, $\Lambda(p) \geq \lambda^*[B]$, yields

$$\lambda^*[B] \leq \Lambda(p) \quad (18)$$

$$\leq \frac{(1 + \xi)^2}{(1 - \xi)^2} \theta(f) \quad (19)$$

$$\leq (1 + \eta)\lambda(f) \quad (20)$$

$$\leq \frac{\lambda(f)}{(1 - \eta)}, \quad (21)$$

(22)

thus concluding the proof. \square

Remark. In approximating $\Lambda(p)$, Algorithms 2 and 3 resort to the sampling-based subroutine as a proxy measure since direct approaches are computationally prohibitive. Though efficient, this sampling procedure does not necessarily guarantee that the assumption $\sum_{j=1}^n p_j f_j^t(\hat{x}) \geq (1 - \xi)\Lambda(p)$ of Lemma 1 holds. Yet, for the current application and settings, this condition tends to be oftentimes satisfied through sufficiently large sample cohorts, hence the empirical success of Algorithms 2 and 3.

ACKNOWLEDGMENTS

We gratefully acknowledge the valuable comments and suggestions provided by the ACM BuildSys 2018 program committee chairs (Polly Huang and Marta Gonzalez), shepherd (Romil Bhardwaj), and anonymous reviewers.

REFERENCES

- [1] Muhammad Aftab, Chien Chen, Chi-Kin Chau, and Talal Rahwan. 2017. Automatic HVAC control with real-time occupancy recognition and simulation-guided model predictive control in low-cost embedded system. *Energy and Buildings* 154 (2017), 141–156.
- [2] Simon H. A. Begemann, Ariadne D. Tenner, and Gerrit J. Van Den Beld. 1998. Lighting System for Controlling the Color Temperature of Artificial Light under the Influence of the Daylight Level. US Patent 5,721,471.
- [3] Dimitris Bertsimas and Santosh Vempala. 2004. Solving convex programs by random walks. *Journal of the ACM* 51, 4 (2004), 540–556.
- [4] Peter Robert Boyce. 2014. *Human Factors in Lighting*. CRC Press.
- [5] D. Caicedo, S. Li, and A. Pandharipande. 2017. Smart lighting control with workspace and ceiling sensors. *Lighting Research & Technology* 49, 4 (2017), 446–460.
- [6] Meghan Clark. 2018. Python Library for Accessing LIFX Devices Locally Using the Official LIFX LAN Protocol. Retrieved from <https://github.com/mclarklk/lifxlan>.
- [7] M. D. Grigoriadis, L. G. Khachiyan, L. Porkolab, and J. Villavicencio. 2001. Approximate max-min resource sharing for structured concave optimization. *SIAM Journal on Optimization* 11, 4 (2001), 1081–1091.
- [8] Adam Kalai and Santosh Vempala. 2006. Simulated annealing for convex optimization. *Mathematics of Operations Research* 31, 2 (2006), 253–266.
- [9] Areg Karapetyan, Sid Chi-Kin Chau, Khaled Elbassioni, Majid Khanji, and Emad Dababseh. 2018. Smart lighting control using oblivious mobile sensors. In *Proceedings of the 5th Conference on Systems for Built Environments (BuildSys'18)*. ACM, New York, NY, 158–167. DOI : <https://doi.org/10.1145/3276774.3276788>
- [10] M. T. Koroglu and K. M. Passino. 2014. Illumination balancing algorithm for smart lights. *IEEE Transactions on Control Systems Technology* 22, 2 (March 2014), 557–567.
- [11] László Lovász and Santosh Vempala. 2004. Hit-and-run from a corner. In *ACM Symposium on Theory of Computing (STOC'04)*. 310–314.
- [12] László Lovász and Santosh Vempala. 2006. Fast algorithms for logconcave functions: Sampling, rounding, integration and optimization. In *IEEE Annual Symposium on Foundations of Computer Science (FOCS'06)*. 57–68.
- [13] László Lovász and Santosh Vempala. 2006. Hit-and-run from a corner. *SIAM Journal on Computing* 35, 4 (2006), 985–1005.
- [14] M. Miki, A. Amamiya, and T. Hiroyasu. 2007. Distributed optimal control of lighting based on stochastic hill climbing method with variable neighborhood. In *2007 IEEE International Conference on Systems, Man and Cybernetics*. 1676–1680. DOI : <https://doi.org/10.1109/ICSMC.2007.4413957>
- [15] Dennis E. Phillips, Rui Tan, Mohammad-Mahdi Moazzami, Guoliang Xing, Jinzhu Chen, and David K. Y. Yau. 2013. Supero: A sensor system for unsupervised residential power usage monitoring. In *IEEE International Conference on Pervasive Computing and Communications (PerCom'13)*.
- [16] Vipul Singhvi, Andreas Krause, Carlos Guestrin, James H. Garrett Jr., and H. Scott Matthews. 2005. Intelligent light control using sensor networks. In *ACM Conference on Embedded Networked Sensor Systems (SenSys'05)*.
- [17] Noah A. Smith and Roy W. Tromble. 2004. Sampling uniformly from the unit simplex. *Johns Hopkins University, Technical Rep* 29 (2004).
- [18] Niels van de Meughevel, Ashish Pandharipande, David Caicedo, and P. P. J. Van Den Hof. 2014. Distributed lighting control with daylight and occupancy adaptation. *Energy and Buildings* 75 (2014), 321–329.
- [19] Yao-Jung Wen and A. M. Agogino. 2008. Wireless networked lighting systems for optimizing energy savings and user satisfaction. In *IEEE Wireless Hive Networks Conference*. 1–7.
- [20] Y.-J. Wen and A. M. Agogino. 2011. Control of wireless-networked lighting in open-plan offices. *Lighting Research & Technology* 43, 2 (2011), 235–248.
- [21] Lun-Wu Yeh, Che-Yen Lu, Chi-Wai Kou, Yu-Chee Tseng, and Chih-Wei Yi. 2010. Autonomous light control by wireless sensor and actuator networks. *IEEE Sensors Journal* 10, 6 (2010), 1029–1041.
- [22] S. A. R. Zaidi, A. Imran, D. C. McLernon, and M. Ghogho. 2014. Enabling IoT empowered smart lighting solutions: A communication theoretic perspective. In *2014 IEEE Wireless Communications and Networking Conference Workshops (WCNCW'14)*. 140–144. DOI : <https://doi.org/10.1109/WCNCW.2014.6934875>
- [23] Nan Zhao, Matthew Aldrich, Christoph F. Reinhart, and Joseph A. Paradiso. 2015. A multidimensional continuous contextual lighting control system using google glass. In *ACM International Conference on Embedded Systems for Energy-Efficient Built Environments (BuildSys'15)*. 235–244.

Received March 2019; revised October 2019; accepted October 2019